AIAA 80-0780R

Honeycomb Sandwich Joints for Primary Structure

Uri Soudak*
Israeli Aircraft Industries, Ltd., Ben Gurion Airport, Israel
and
Robert A. Hamm†
Boeing Commercial Airplane Company, Seattle, Wash.

Analysis methods and joint design details have been developed for adhesively bonded aluminum honeycomb in aircraft primary structure. Joint design details that were tested for strength, durability, and environmental resistance provide a low-cost design that is structurally efficient and durable. Weight and cost savings, producibility, and durability have been confirmed by five years of service experience on the YC-14 empennage primary structure. The analysis considers the effect of the core on face sheet stress, the effect of face sheet eccentricity, and a failure analysis method for square-edge panels. In addition, it allows strength/weight optimization procedures for honeycomb design.

Nomenclature

b	= panel width
C	= core depth
d	= one half the distance between the skin centroids
E_{cc}	= core flatwise modulus of elasticity
F_{peel}, M_{peel}	= end tension load or end moment needed to produce core peel at the square edge
F_{crush}, M_{crush}	= end compression load or end moment needed to produce core crushing at the square edge
F_{shear}, M_{shear}	= end load or end moment needed to produce core shear
F_{cc}	= core flatwise strength
F_{sL}/F_{sW}	= core shear strength (L or W direction)
G_L/G_W	= core shear modulus of elasticity
G_{xy}	= outer skin shear modulus of elasticity
K	= factor for tension loads. It will vary for different adhesives and for different materials and equals one for compression.
n	= half-core length between square edges
S	$= E_{cc}\left(\frac{1}{G_L C^2} + \frac{1}{G_{xy} t_1^2}\right)$
t_1	= outer skin gage (average)
t_2	= inner skin gage

Introduction

ALUMINUM honeycomb sandwich construction has been used in aircraft secondary structure applications for many years. The early use of aluminum honeycomb in these secondary parts such as wing trailing edge panels and spoilers resulted in unsatisfactory service experience. Part failures because of moisture-induced corrosion and subsequent delaminations resulted in a bad reputation for bonded structure.

Beginning around 1965, many improvements were made that systematically eliminated the durability problems of bonded aluminum honeycomb structures. Some of these improvements were elimination of perforated core and introduction of corrosion resistant core, elimination of the use of clad aluminum in bonded assemblies, introduction of phosphoric acid-anodized surface preparation, use of primers containing corrosion resistant chromates, and use of new durable adhesives. Extensive laboratory tests and limited service experience (5 yr) show the new bonding technology to be tough, durable, and highly tolerant to environmental exposure.

Early bonding failures prevented the use of aluminum honeycomb in aircraft primary structure; the failure of primary structure could result in the loss of the aircraft. To be considered for use in primary structure, a material must show cost and weight effectiveness, allow for ease of repair, as well as being strong, durable, and environmentally resistant. Finally, the structure must yield consistently and predictably to some form of analysis. This paper deals with the development of design details and semiempirical analysis methods necessary to design aluminum honeycomb aircraft primary structure.

YC-14 Development Program

The theoretical structural efficiency of adhesively bonded aluminum honeycomb is high compared to conventional skin/stringer design for many applications. Figure 1 shows aluminum honeycomb with the highest strength-to-weight ratio of the considered design concepts in the range of 1-15 kips/in. It is this potential for weight savings and high strength that stimulates the search for practical design details and analysis methods that will enable the use of aluminum honeycomb in primary structure.

Because the design loads in the empennage of a jet transport fell within the range of honeycomb supremacy, this type of structure was chosen for the YC-14 prototype design. An extensive design development program was initiated in

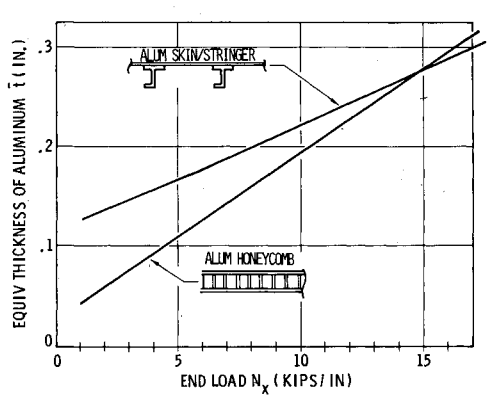

Fig. 1 Structural efficiency comparison.

Presented as Paper 80-0780 at the AIAA/ASME/ASCE/AHS 21st Structures, Structural Dynamics and Materials Conference, Seattle, Wash., May 12-14, 1980; submitted June 10, 1980; revision received March 24, 1981.

*Supervisor, Structures Design.

†Design Specialist.

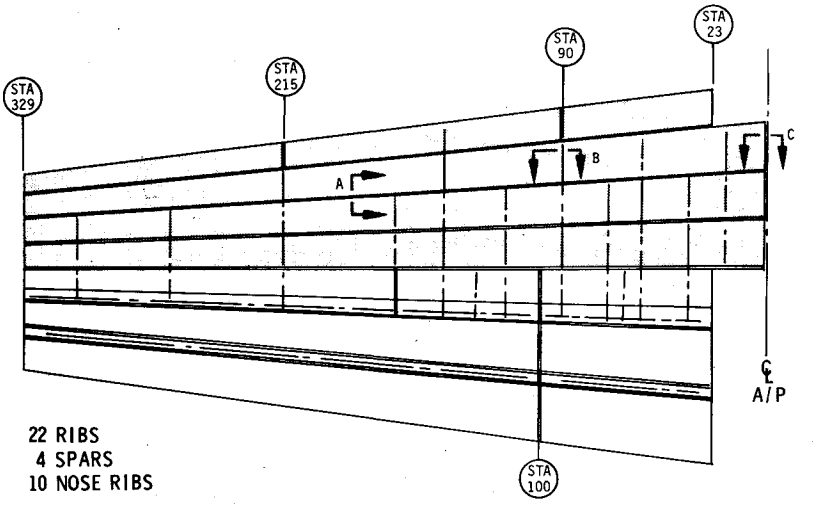

Fig. 2 YC-14 stabilizer honeycomb box.

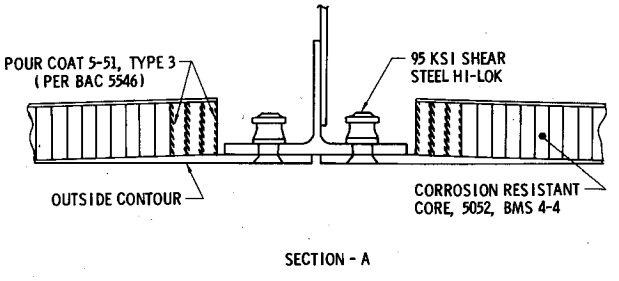

Fig. 3 Honeycomb panel over spar.

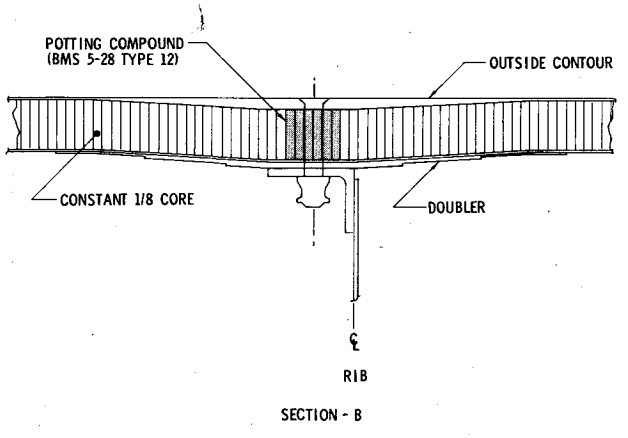

Fig. 4 Honeycomb panel over rib.

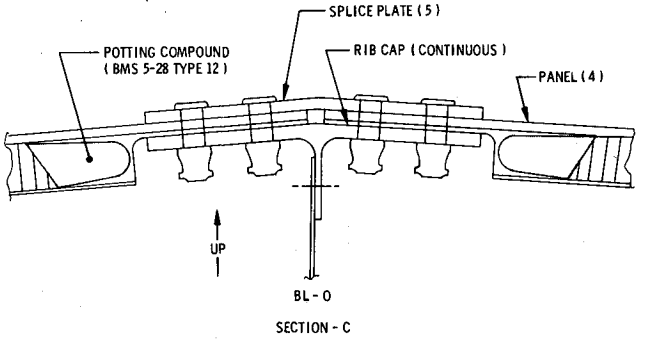

Fig. 5 Stabilizer BL 0 splice.

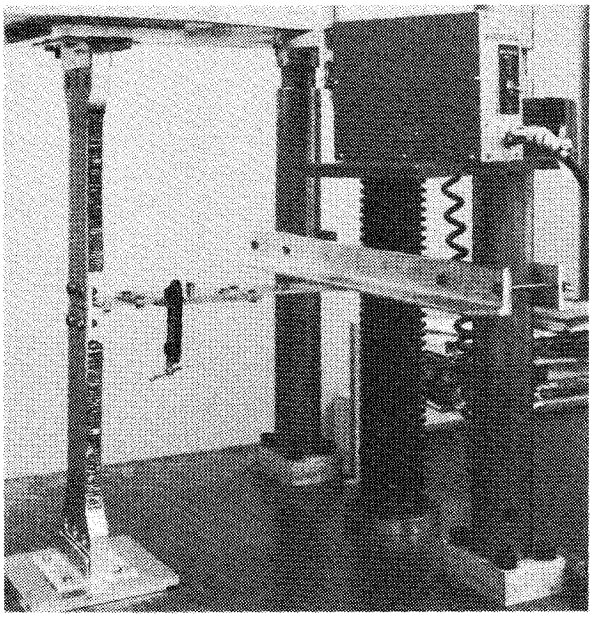

Fig. 6 Test setup.

support of the YC-14 design. Figure 2 shows the structure used in the horizontal stabilizer of the YC-14 prototype.

Actual honeycomb structure deviates from theoretical structure at the attachment edges and points of concentrated load introduction. Continuous honeycomb, represented by the skin to rib attachment in Fig. 4, is highly efficient, but must sacrifice some weight to potting compound or dense core at the rib crossover in order to take compressive and fastener clamp-up loads. Edge attachments, represented by Figs. 3 and 5, are much less efficient because of their high eccentricity. The square-edge attachment shown in Fig. 3 is typical of a skin-to-spar attachment and is the lightest weight design where loads normal to the edge are low and the primary loads are parallel to the edge. When the loads normal to the edge are high, as at the skin panel splices at the root of the horizontal stabilizer (Fig. 5), the edge attachments must be heavier to avoid buckling and take the secondary bending effects.

The development program consisted of panel tests and a large amount of testing on edge attachments and joints representative of continuous, square-edge, and pickle-fork or reinforced-edge structure. A typical test specimen and setup is shown in Fig. 6. Over a hundred specimens were tested in tension and compression for static strength, fatigue strength, and environmental resistance.

The primary results of the tests were that the square-edge joint design is weight efficient up to 3-4 kips/in. load. At higher loads (up to 8 kips/in. were used) the continuous core joint was the best design. A significant result was that the simpler joint obtained the better result. In the static and fatigue tests, the best joint featured only bonding with no fasteners, i.e., a rib or a spar bonded directly to the inner skin of a sandwich skin.

Analysis

Failure Modes

Honeycomb sandwich panels may fail in several different modes. Continuous-core unstable modes are general buckling, shear crimping, and face wrinkling. These failure modes are a function of core strength. Analyses of unstable cases are available in technical literature. Spliced-core sandwich tests conducted at Boeing showed one exception to the general theories—it was found that core splices considerably reduce the shear-crimping strength of the assembly.

Interrupted-core (square-edge) panels do not manifest any of the above-mentioned unstable modes. Buckling is always local, at the core edge, because of the abrupt change in the section area. As to the stable failure modes, panel strength is highly affected by the core strength and bonding flatwise strength. These facts were demonstrated in numerous tests.

Core Effect

Existing theories do not allow any participation of the core in carrying axial or bending loads. The core carries shear loads and has a stabilization effect for axial compression loads.

Tests performed at Boeing showed a high participation of the core in carrying axial and bending loads when the face sheets were in the plastic range and the core was still elastic.

A special test series was planned to evaluate the core effect. Specimens were built with and without core, using the same sheet metals for skins and the same bonding processes. Specimens were loaded in pure tension at exactly the same conditions. The specimens with 3.1 lb/ft^3 core manifested 4% ultimate strength increase, and those with 6.1 lb/ft^3 core showed an 8% increase compared to the specimens with bonded sheet metal without any core. In the elastic range, the yield strength was increased from 0.5-1% when the core was present.

These results are attributed to the following two factors:

1) The core has a small capability of carrying axial loads while bonded to the skins. This capability is increased significantly when the skins are in the plastic range and the core is still elastic.

2) The core decreases the necking of the critical section, resulting in lower stress at the skins for a given load.

In cases where a panel is loaded axially away from its neutral axis, bending occurs and the small core effect has a large contribution to reduce the bending as it shifts the neutral axis position to reduce the eccentricity. Specimens that have a 2:1 ratio of outer to inner skin, and are loaded at the center of the panel edge, failed in the inner skin at about 200% of the predicted ultimate load, calculated with no core effect.

To account for the core effect in the analysis, the load distribution factors (α,β,γ), the sandwich moment of inertia (I), and neutral axis locations (e_1,e_2) are determined (sandwich panel only without chords) by the following equations:

$$\alpha=\frac{t_1}{t_1+t_2+CE_c/E}$$

$$\beta=\frac{t_2}{t_1+t_2+CE_c/E}$$

$$\gamma=\frac{CE_c/E}{t_1+t_2+CE_c/E}$$

For compression only. For tension loads, use KE_c in place of E_c, where K is an empirical constant.

$$d=\frac{1}{2}\left[C+\frac{t_1+t_2}{2}\right]$$

$$e_1+e_2=2d$$

e_1 is determined from the solution of the following:

For compression at t_2,

$$e_1^2(K-1)\frac{E_c}{E}+e_1\left[2\left(t_1+t_2+C\frac{E_c}{E}-\frac{K-1}{2}t_1\frac{E_c}{E}\right)\right]+\left[-4dt_2\left(1-\frac{E_c}{2E}\right)-4d^2\frac{E_c}{E}\right]=0$$

For tension at t_2,

$$e_1(K-1)\frac{E_c}{E}+e_1\left[-2\left(t_1+t_2+KC\frac{E_c}{E}+\frac{K-1}{2}t_1\frac{E_c}{E}\right)\right]+\left[4dt_2\left(1-\frac{K}{2}\frac{E_c}{E}\right)+4d^2K\frac{E_c}{E}\right]=0$$

I is determined from the equations:

For compression at t_2,

$$\frac{I}{b}=(t_1e_1^2+t_2e_2^2)+\frac{E_c}{E}\left[\frac{1}{3}\left(e_2-\frac{t_2}{2}\right)^3+K\frac{1}{3}\left(e_1-\frac{t_1}{2}\right)^3\right]$$

For tension at t_2,

$$\frac{I}{b}=(t_1e_2^2+t_2e_2^2)+\frac{E_c}{E}\left[\frac{1}{3}K\left(e_2-\frac{t_2}{2}\right)^3+\frac{1}{3}\left(e_1-\frac{t_1}{2}\right)^3\right]$$

Square-Edge Analysis

Square-edge specimen tests showed different failure modes—edge peel, edge crush, core shear, and local edge buckling. It was found that slight changes in skin gages and core density have major effects on the structural strength.

A mathematical model (Fig. 7) was created to simulate the structure. The model is based on the following:

1) Skins and core are elastic.

2) The core may participate in axial loading as demonstrated by core effect tests.

3) Eccentricity at the edge is balanced by shear in the core.

4) Shear in the core must be balanced by a peel or crush load (depending upon external load configuration) at the square edge, internal in the structure, between the core and the outer skin.

5) The peel or crush load is a distributed load with a high, yet unknown, concentration at the edge.

Models with pure tension or compression, pure bending, and pure vertical (out-of-plane) shear are thus set, and any combination of these loads has a linear effect in the elastic range.

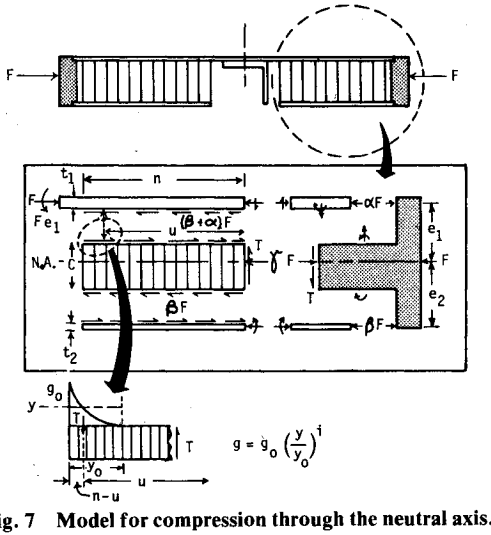

Fig. 7 Model for compression through the neutral axis.

The model was analyzed using the minimum elastic energy method and a good correlation was found by using only one term of the type $g=g_0(y/y_0)^i$ to represent the peel or crush-load distribution.

Although this type of representation tends to diverge, a finite stable solution is obtained for the maximum stress at the core edge and for the core shear. Note that the peel stress depends on the bond flatwise strength, while the crush strength is a function of the core flatwise strength.

The design formulas are derived from the model as follows:

$$T+\int_0^{y_0} g\,dy=\frac{g_0}{(i+1)y_0^i}y^{(i+1)}\Big|_0^{y=y_0}=\frac{1}{(i+1)}g_0y_0$$

$$y_0-(n-u)=\frac{1}{T}\int_0^{y_0} gy\,dy=\frac{1}{T}\frac{g_0y_0^2}{(i+2)}=\frac{i+1}{i+2}y_0$$

Thus,

$$y_0=(i+2)(n-u)\qquad T=g_0\frac{i+2}{i+1}(n-u)$$

The compression energy exerted by g on the outer face sheet can be neglected, compared to that exerted on the core or adhesive for most sandwich panels, since

$$E_{\text{skin}}\gg E_{cc\,\text{core}}$$

For tension,

$$E_{\text{skin}}\gg E_{\text{adhesive}}$$

For aluminum,

$$E_{\text{skin}}=10.5\times10^6\text{ psi}\qquad E_{cc}\geq4.0\times10^5\text{ psi}$$

The shear energies of core and skin are of the same order of magnitude since

$$(t^2G_{xy})_{\text{skin}}\cong(C^2G_L)_{\text{core}}$$

Designating,

W_1 = core crushing energy
W_2 = core shear energy
W_3 = outer-skin shear energy
$W_1+W_2+W_3=\min$

$$W_1=\int_0^{y_0} gE\,dy=\frac{1}{E}\int_0^{y_0} g^2\,dy=\frac{1}{E}\frac{g_0^2y_0}{(2i+1)}$$

In order to obtain the shear energy, the core length n is divided into two regions. In the first, the shear load increases from zero at the edge to T at $n-y_0$. Beyond that point, it is constant.

$$T_1=T-\int g\,dy=\frac{g_0}{(i+1)}\left(y_0-\frac{1}{y_0^i}y^{(i+1)}\right)$$

$$T_2=T$$

$$W_2=\frac{1}{G_LC^2}\left(\int_0^{n-y_0} T^2\,dy+\int_{n-y_0}^{n} T_1^2\,dy\right)$$

$$W_2=\frac{1}{G_LC^2}\frac{1}{(i+1)^2}g_0^2y_0^2\left(n-y_0\frac{3i+4}{(i+2)(2i+3)}\right)$$

$$W_3=W_2\frac{G_LC^2}{G_{xy}t_1^2}$$

To formulate W as a function of U and i only, substitute y_0, g_0, and T using

$$y_0=(i+2)(n-u)$$

$$g_0=T\frac{(i+1)}{(i+2)}\frac{1}{(n-u)}$$

$$T=\frac{F[\beta C+\gamma(e_1-t_1/2)]}{u}=\frac{C_0}{u}$$

The result is

$$\frac{E_{cc}}{C_0^2}W=\frac{(i+1)^2}{u^2(n-u)(2i+1)(i+2)}+S\left(\frac{1}{u^2(2i+3)}[i(3u-n)+(4u-n)]\right)$$

where

$$S_{\text{comp}}=E_{cc}\left(\frac{1}{G_LC^2}+\frac{1}{G_{xy}t_1^2}\right)$$

$$S_{\text{tens}}=E_A\left(\frac{1}{G_LC^2}+\frac{1}{G_{xy}t_1^2}\right)$$

As i and u are independent variables, the energy is to be minimized with respect to each

$$\frac{dW}{di}=0\qquad\frac{dW}{du}=0$$

Differentiating with respect to i, W is minimum at $i=\infty$, which means that $y_0=\infty$, an infinite plate. The solution is first found for an infinite plate, and then the solution for finite plates is developed.

Substituting $i=\infty$ in the energy equation,

$$\frac{E_{cc}}{C_0^2}W=\frac{1}{2}\frac{1}{u^2(n-u)}+\frac{3u-n}{2u^2}S=\min$$

$$\frac{dW}{du}=0$$

$$3u-2n+S(n-u)^2(2n-3u)=0$$

$$(3u-2n)[1-S(n-u)^2]=0$$

$$u_1=\frac{2}{3}n,\qquad u_2=n-\sqrt{1/S}$$

Checking for minimum,

$$\frac{d^2W}{du^2}>0$$

which is satisfied only for u_2. Thus,

$$n-u=\left\{\left[E_{cc}\left(\frac{1}{G_LC^2}+\frac{1}{G_{xy}t_1^2}\right)\right]^{-1}\right\}^{1/2}$$

This equation is a first approximation for long panels. A better approximation is developed below as an aid in determining when to use the simple approximate solution and when the complicated one is necessary.

For finite plates, y_0 max value is n

$$y_0=(i+2)(n-u)=n\qquad i=\frac{2u-n}{n-u}$$

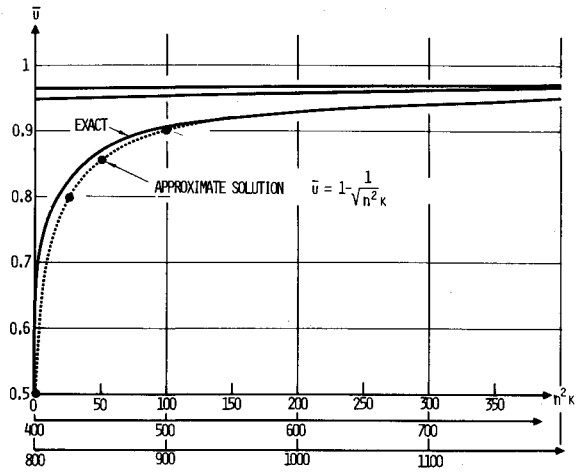

Fig. 8 Approximate and exact solutions for *U*.

Substituting i in the energy equation,

$$\frac{E_{cc}W}{C_0^2} = \frac{1}{n(n-u)(3u-n)}$$

$$+S\frac{(2u-n)(3u-n)+(n-u)(4u-n)}{u^2(n+u)} = \min$$

$$\frac{dW}{du} = 0$$

$$(n+u)^2(3u-2n) - Sn(n-u)^2(3u-n)^2 = 0$$

or

$$(1+\bar{u})^2(3\bar{u}-2) - Sn^2(1-\bar{u})^2(3\bar{u}-1)^2 = 0$$

where $\bar{u} = u/n$. This equation for $\bar{u}$ is of the fourth order and its solution is presented in Fig. 8.

Note that for values of $Sn^2 > 150$, the solution for an infinite plate is also good for finite plates. The main formulas are listed below:

$$F_{\text{peel/crush}} = bF_{cc}\frac{n(t_2+t_1)}{t_2C\sqrt{S}}K$$

$$F_{\text{shear}} = F_{sL/W}\frac{b(t_2+t_1)}{t_2}\left(n-\frac{1}{\sqrt{S}}\right)$$

$$M_{\text{peel/crush}} = bF_{cc}\frac{nd}{C\sqrt{S}}K$$

$$M_{\text{shear}} = F_{sL/W}bd\left(n-\frac{1}{\sqrt{S}}\right)$$

Using these equations, the square-edge design can be optimized to avoid shear failure or edge failure, thus achieving the continuous-core strength with less cost and less weight. Axial compression cannot obtain an equivalent strength because local buckling of the outer skin at the edge occurs at about 50% of the load that buckles the continuous-core panels. Analysis methods for square-edge designs with tension, bending, and transverse shear were also developed using similar methods. Continuous-core specimens were also tested and analysis methods derived that account for face sheet eccentricity and core effect.

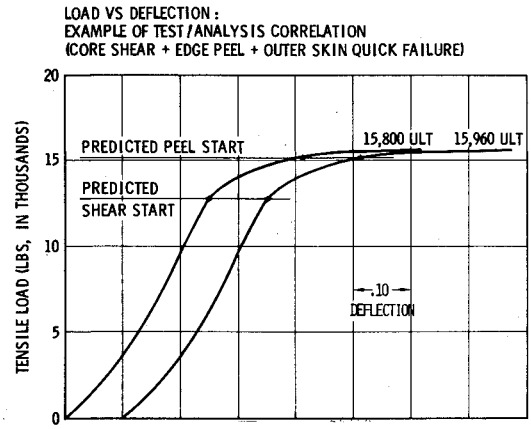

Fig. 9 Edge peel test/analysis correlation.

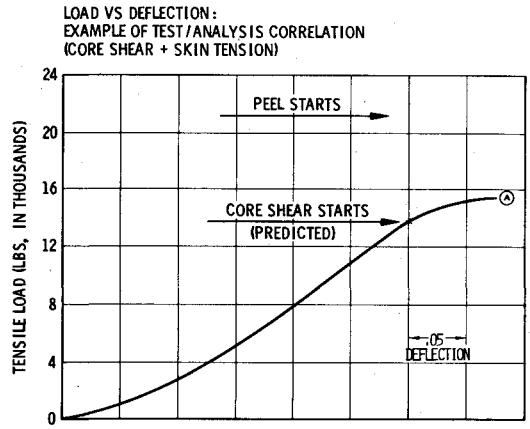

Fig. 10 Core shear test/analysis correlation.

Test and Analysis Correlation

The analysis methods described herein apply to initial failures only, such as core shear or edge peel. The honeycomb specimens continue to carry loads above these failure values to ultimate two-piece failures. The analysis methods successfully predicted the failure modes of the test specimens. The calculated lowest initial failure of the specimens (F_{shear}, F_{crush}, etc.) corresponded well with the knee of the load/deflection diagrams of the specimens as shown in Figs. 9 and 10.

Figure 9 is the load/deflection curve for two square-edge design specimens tested in tension. The initial failure was core shear with a subsequent peel failure at the square edge and an ultimate skin tension failure. All three failures modes were apparent in the specimen. The initial core shear failure corresponds well with the knee of the load/deflection curve.

Figure 10 is the load/deflection curve for an improved peel design with a dense core insert at the square edge. This specimen did not exhibit the distinctive peel failure and corresponded well with the analysis. The analysis methods correctly predicted failure modes and levels in the specimens analyzed.

Concluding Remarks

The technology for using adhesively bonded aluminum honeycomb in an aircraft primary structure is available. Two YC-14 prototype aircraft continue to add flight hours and credibility to honeycomb durability. In summary, aluminum honeycomb is lightweight, durable, and structurally predictable.